Clays and Clay Minerals, Vol. 46, No. 3, 240–244, 1998.

MOLECULAR SIMULATIONS OF MONTMORILLONITE INTERCALATED WITH ALUMINUM COMPLEX CATIONS. PART II: INTERCALATION WITH $Al(OH)_3$-FRAGMENT POLYMERS

P. ČAPKOVÁ,[1,2] R. A. J. DRIESSEN,[1] M. NUMAN,[1] H. SCHENK,[1] Z. WEISS[3] AND Z. KLIKA[3]

[1] Laboratory of Crystallography, AIMS, University of Amsterdam, Nieuwe Achtergracht 166, 1018 WV Amsterdam, The Netherlands

[2] Faculty of Mathematics and Physics, Charles University Prague, Ke Karlovu 5, 12116 Prague, Czech Republic

[3] Central Analytical Laboratory, Technical University Ostrava, 70833 Ostrava, Czech Republic

Abstract—The Crystal Packer module in the Cerius[2] modeling environment has been used to study the structure of montmorillonite intercalated with $Al(OH)_3$-fragment (gibbsite-like) polymers. Basal spacings in gibbsite-like polymers arranged in 2 layers in the interlayer of montmorillonite varied in the range 19.54–20.13 Å, depending on the type and arrangement of $Al(OH)_3$ fragments. The inhomogeneous distribution of intercalating species in the interlayer and, consequently, the turbostratic stacking of layers has been found for gibbsite-like polymers as well as in the case of Keggin cations (Čapková et al. 1998). The dominating contribution to the total sublimation energy comes from electrostatic interactions for both intercalating species, gibbsite-like polymers and Keggin cations.

Key Words—Al-Cation, Gibbsite-like Polymers, Intercalation, Molecular Simulations, Montmorillonite.

INTRODUCTION

Many recent structure investigations of clay minerals intercalated with Al-OH polymers focused on the nature of the intercalating agent (Plee et al. 1987; Hsu 1992; Schoonheydt et al. 1993, 1994; Dubbin et al. 1994). The ^{27}Al nuclear magnetic resonance (NMR) spectra of the intercalating solutions normally show the presence of 2 species: octahedral Al and tetrahedral Al, included in Al_{13} oligomer-Keggin cation (Figueras et al. 1990; Hsu 1992; Schoonheydt et al. 1994). Although the Keggin cation has been a widely accepted intercalating species, Schoonheydt and Leehman (1992) and Hsu (1992) showed that intercalation is also possible with concentrated Al-OH solutions in which the Keggin cation is almost totaly absent. Hsu (1988) proposed for Al-OH polymers the hexagonal-ring structure resembling fragments of $Al(OH)_3$ crystals. He prepared 2 different types of Al-OH solutions for intercalation of smectites and vermiculites: 1) one dominated by octahedral Al, ascribed to gibbsite-like polymers and 2) one dominated by Keggin cations (Hsu 1992). The results of intercalation showed that both intercalating agents lead to the same basal spacing of intercalated smectites, $d(001)$ = 19 Å. Based on these results, Hsu (1992) proposed the model of intercalated smectite with 2 layers of $Al(OH)_3$-fragment polymers in the interlayer.

The aim of the present work is to obtain the detailed model of the montmorillonite structure intercalated with gibbsite-like fragments. The Cerius[2] modeling environment has been used to investigate the intercalant-layer bonding and the structural parameters important for sorption properties of this intercalate. The montmorillonite structures intercalated with Keggin cation and with gibbsite-like polymers were compared on the base of present molecular simulations.

MODELING WITH $Al(OH)_3$-FRAGMENT POLYMERS

The Crystal Packer module in the Cerius[2] modeling environment has been used in the present calculations. That means the nonbonded intercations van der Waals (VDW), coulombic (COUL) and hydrogen bonding (HB) have been taken into account. (For a more detailed description of the Crystal Packer module, see Čapková et al. 1998). The initial model of the 2:1 layer of montmorillonite (MMT) was built using the PLUVA 2.3 program (Driessen et al. 1988) and the structural data for montmorillonite according to Tsipursky and Drits (1984) (space group $C2/m$). The unit cell parameters given by Méring and Oberlin (1967), a = 5.208 Å and b = 9.02 Å have been used. The composition of 1 unit cell (further denoted as MMT) in the 2:1 silicate layer corresponds to the formula $(Al_3Mg_1)Si_8O_{20}(OH)_4$; that is, 1 MMT unit cell carries the charge (−1). The supercell containing the 6-MMT unit was built for all models with different gibbsite-like fragments used in the present calculations. The 6-MMT supercell parameters were:

$A = 3a$ = 15.62 Å (fixed during energy minimization),

$B = 2b$ = 18.04 Å (fixed during energy minimization),

C, variable (C-axis perpendicular to sheets), $\gamma = 90°$ fixed, α and β variable.

Copyright © 1998, The Clay Minerals Society

https://doi.org/10.1346/CCMN.1998.0460303 Published online by Cambridge University Press

Table 1. Basal spacings, $d(001)$, and the average values of van der Waals, coulombic, hydrogen bond and total sublimation energy, E_s, per supercell for various models of montmorillonite intercalated with gibbsite-like polymers.

Intercalants in 6-MMT supercell	Single-ring 1 layer Model I	Double-ring 1 layer Model II	Single-ring sandwich Model III	Double-ring sandwich Model IV	Double-ring shifted Model V
d-spacing (Å)	14.58	14.18	19.94	20.06	19.58
VDW (kcal/mol)	134.3	166.4	140.9	194.8	199.7
COUL (kcal/mol)	2984.9	3145.2	2307.5	2095.0	3057.8
HB (kcal/mol)	29.7	48.0	37.6	59.4	64.1
E_s (kcal/mol)	3148.9	3359.6	2486.0	2349.2	3321.6

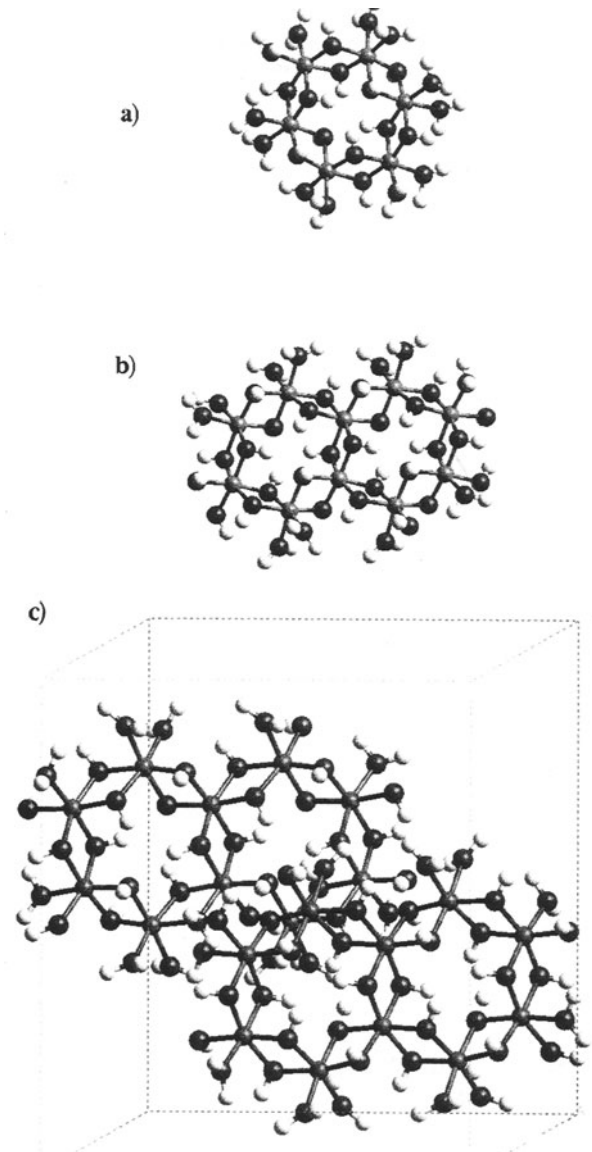


Figure 1. Intercalating species built from the gibbsite structure fragments: a) Single 6-member ring $[Al_6(OH)_{12}(H_2O)_{12}]^{6+}$; b) Double ring $[Al_{10}(OH)_{24}(H_2O)_{14}]^{6+}$; c) Double rings arranged in 2 mutually shifted layers (Model V), resulting in small overlap and, consequently, small repulsion forces between double rings in the lower and upper layer.

The intercalating species $Al(OH)_3$-fragment polymers were extracted from the $Al(OH)_3$-gibbsite structure (Saalfeld and Wedde 1974). To balance the layer charge (−6), the following intercalating species have been inserted in the interlayer of the 6-MMT supercell:

1) Model I: single 6-member ring $[Al_6(OH)_{12}(H_2O)_{12}]^{6+}$ (Figure 1a).
2) Model II: double-ring $[Al_{10}(OH)_{24}(H_2O)_{14}]^{6+}$ (Figure 1b). To keep the charge of the complex cation (6+), the original single rings from Figure 1a have been partially hydrolyzed.
3) Model III: single-ring sandwich $[Al_{12}(OH)_{30}(H_2O)_{18}]^{6+}$, consisting of 2 partially hydrolyzed single rings $[Al_6(OH)_{15}(H_2O)_9]^{3+}$ arranged in 2 layers, as shown in Figure 2.
4) Model IV: double-ring sandwich $[Al_{20}(OH)_{54}(H_2O)_{22}]^{6+}$; that is, 2 partially hydrolyzed double rings $[Al_{10}(OH)_{27}(H_2O)_{11}]^{3+}$ are arranged in 2 identical layers in the interlayer.

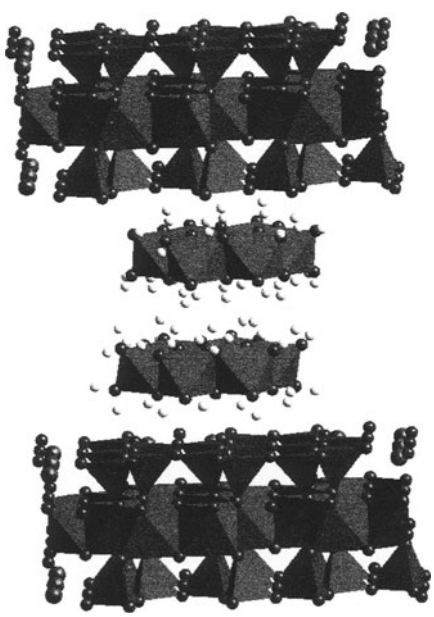


Figure 2. Calculated crystal packing for the single-ring sandwich $[Al_{12}(OH)_{30}(H_2O)_{18}]^{6+}$ in the 6-MMT supercell (Model III), $d(001)$ = 19.94 Å.

https://doi.org/10.1346/CCMN.1998.0460303 Published online by Cambridge University Press

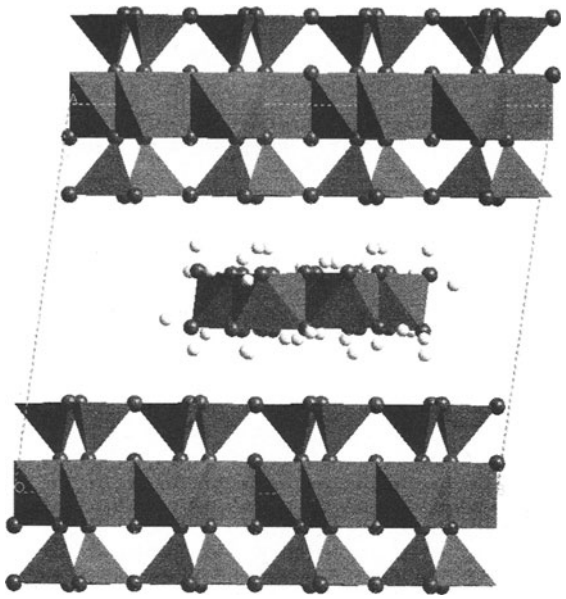


Figure 3. The most stable crystal packing with the single ring $[Al_6(OH)_{12}(H_2O)_{12}]^{6+}$ in the 6-MMT supercell, $d(001)$ = 14.58 Å.

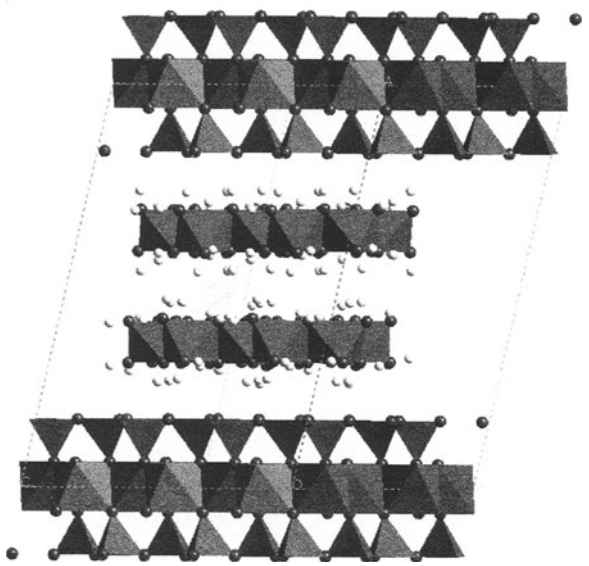


Figure 4. Calculated crystal packing for the double-ring sandwich $[Al_{20}(OH)_{54}(H_2O)_{22}]^{6+}$ in the 6-MMT supercell (Model IV), $d(001)$ = 20.06 Å.

5) Model V: $[Al_{20}(OH)_{54}(H_2O)_{22}]^{6+}$-double rings $[Al_{10}(OH)_{27}(H_2O)_{11}]^{3+}$, arranged in 2 mutually shifted layers resulting in a small overlap of double rings, as shown in Figure 1c.

The strategy of modeling using the Crystal Packer module was similar to Čapková et al. (1998) for the case of Keggin cations in the interlayer. The supercell was divided into the following rigid units:

1) Two rigid units were assigned to the supercell in models I and II: silicate layer and single ring (Model I) and silicate layer and double ring (Model II).

2) The initial models III, IV and V consisted of 3 rigid units: silicate layers and 2 single rings (Model III) and silicate layer and 2 double rings (models IV and V).

All rigid units could rotate and translate during energy minimization and the nonbonded interactions (VDW, COUL, HB) were calculated between the rigid units. The first minimalization was carried out using external pressure of 99 kbar to get the rigid units into closer contact; then the external pressure was removed to get the final results.

RESULTS AND DISCUSSION

$Al(OH)_3$ Fragments Arranged in 1 Layer: Models I and II

Energy minimization for models I and II led to the most stable crystal packing, where the 6-member rings of hydroxy-aluminum polymers were parallel to the silicate layer (that is, the aluminum planes in rings were parallel to the silicate layers). The result of energy minimization for Model I with the single ring $[Al_6(OH)_{12}(H_2O)_{12}]^{6+}$ in the interlayer is illustrated in Figure 3. The basal spacings obtained for the single ring, $d(001)$ = 14.58 Å, and double ring, $d(001)$ = 14.18 Å, in the interlayer led to the conclusion that in the intercalated smectites with basal spacing ~19 Å, the $Al(OH)_3$-fragment polymers are arranged in 2 layers in the interlayer. This model was already suggested by Hsu (1992) and Dubbin et al. (1994).

The upper and lower oxygen planes of single and double rings are bonded via hydrogen bridges to the silicate layers. The values of VDW, COUL, HB and total sublimation energy per supercell, E_s, are summarized in Table 1. The dominating contribution to E_s comes from the electrostatic interactions. Although both complexes, single- and double-ring, carried the same charge (−6), one can see from Table 1, that the double ring (Figure 1b) in the interlayer leads to higher sublimation energy and, consequently, to lower basal spacing, than the single ring. This can be explained by the more homogeneous charge distribution in the interlayer and an increasing number of hydrogen bridges and VDW interactions in the case of the larger $Al(OH)_3$ fragments.

The translations of gibbsite-like polymers along the silicate layers did not lead to significant changes in the coulombic and total sublimation energy. Changes in COUL and E_s are less than 1%, which indicates that there are no preferences for the single- or double-ring positions in the interlayer and, consequently, no ordering of gibbsite-like polymers in the interlayer. No regular stacking of layers can be expected. The same results, confirming the turbostratic stacking of layers,

https://doi.org/10.1346/CCMN.1998.0460303 Published online by Cambridge University Press

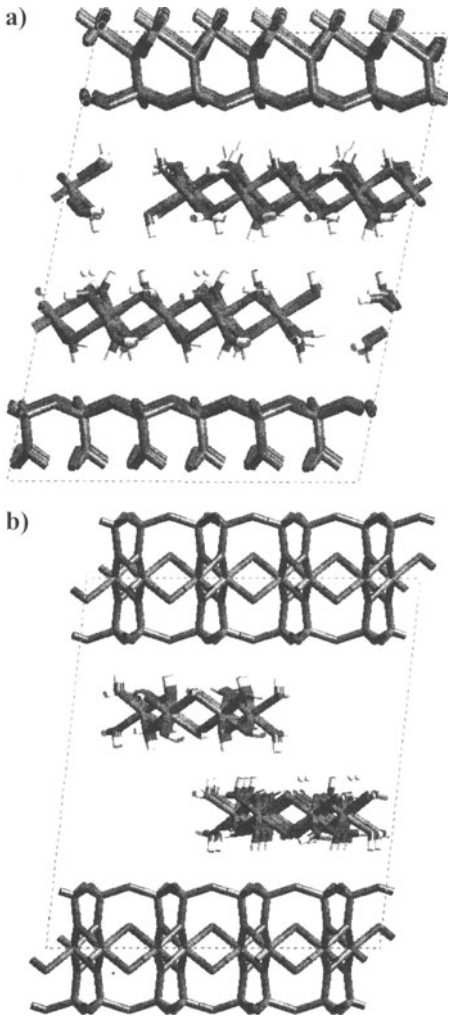


Figure 5. Schematic illustration of crystal packing with shifted double rings arranged in 2 layers in the 6-MMT supercell, a) along *A* direction, b) along *B* direction, (Model V), $d(001)$ = 19.58 Å.

have been obtained for Keggin cations in the interlayer (Čapková et al. 1998).

$Al(OH)_3$ Fragments Arranged in 2 Layers: Models III–V

The result of energy minimization for Model III, with the single-ring sandwich $[Al_{12}(OH)_{30}(H_2O)_{18}]^{6+}$ intercalated into the 6-MMT supercell, is illustrated in Figure 2. The single rings in the sandwich were independent rigid units that can be translated and rotated during energy minimization. As shown in Figure 2, the aluminum planes in the rings are parallel to the silicate layers. Hydrogen bridges occur between the rings and silicate layers and between both rings. The values of basal spacing and energy contributions to E_s are presented in Table 1. The average basal spacing of 19.94 Å obtained for this model is very close to the values obtained for montmorillonite intercalated with the strongly hydrolyzed Keggin cations Al_{13}^{3+} (Čapková et al. 1998, Table 1). The comparison of the values of VDW, COUL, HB and E_s in Table 1 for models I and III (1 single ring with 2 single rings in a sandwich) shows that the coulombic energy and, consequently, the total sublimation energy per supercell is significantly lower in the case of the single-ring sandwich, which indicates the repulsion forces between the single rings.

In model IV with the double-ring sandwich $[Al_{20}(OH)_{54}(H_2O)_{22}]^{6+}$, the average basal spacing $d(001)$ = 20.06 Å is slightly higher than in the case of Model III, as a result of higher repulsion between the double rings than between the single rings. Lower coulombic and, consequently, lower total sublimation energy observed for this model in comparison with Model III supports this explanation (Table 1). Both double rings in the sandwich have aluminum planes parallel to the silicate layers, as shown in Figure 4.

For Model V, with the double rings arranged in 2 mutually shifted layers (Figure 1c), the results were significantly different from models III and IV. The average basal spacing obtained for this model, $d(001)$ = 19.58 Å, is lower than for the single- and double-ring sandwich, while the values of coulombic and total sublimation energy are higher, as shown in Table 1. The small overlap of double rings in Model V reduces the repulsion forces between them, resulting in higher stability of intercalated structure. The orientation of the shifted double rings remains the same as in all other models (I–IV) (that is, Al-planes parallel with the silicate layers). Crystal packing for this case is schematically illustrated in Figure 5 along the *A*, *B* direction. It is evident from Figure 5 that in the most stable crystal packing (Model V), the height of pores in the interlayer is limited by the height of rings.

Comparison of Montmorillonite Structure Intercalated with Keggin Cations and Gibbsite-Like Polymers

Results of molecular simulations obtained for intercalation of Keggin cations and gibbsite-like polymers into montmorillonites exhibit many common features. The character of bonding between cations and silicate layers is the same in both cases, meaning that the dominating contribution to the total sublimation energy comes from the coulombic interactions. Hydrogen bridges link the cations with the silicate layers.

Both intercalating species led to very similar ranges of basal spacings. The full range of basal spacings obtained for Keggin cations in different degrees of hydrolysis was $d(001)$ = 19.38–20.27 Å. For gibbsite-like polymers arranged in 2 layers, the lowest value of 19.54 Å has been found for the shifted double rings (Model V) and the highest value of 20.13 Å for the double-ring sandwich (Model IV). Consequently, iden-

https://doi.org/10.1346/CCMN.1998.0460303 Published online by Cambridge University Press

tification of intercalating species by the diffraction measurements of basal spacing is practically impossible. A similar result has been reported by Hsu (1992), who presented the average value of X-ray diffraction (XRD) basal spacings for smectites intercalated with 1) Keggin cations, $d(001)$ = 19.01 Å and 2) gibbsite-like polymers, $d(001)$ = 19.05 Å.

During the translations of Al-cations along the silicate layers, no preferences have been found for their positions. This means that turbostratic stacking of layers and no 2-dimensional ordering in the interlayer exists for Keggin cations as well as for gibbsite-like polymers.

Comparison of the total sublimation energy per unit cell of montmorillonite for both intercalating species shows the tendency to higher stability of the montmorillonite structure intercalated with gibbsite-like polymers. The total sublimation energy E_s = 3321.6 kcal/mol, for the most stable crystal packing with gibbsite-like polymers arranged in 2 layers (Model V), is higher than the highest value of E_s obtained for Keggin cations Al_{13}^{3+} in the 2 × 3-MMT supercell: E_s = 3136.6 kcal/mol.

The main difference between the montmorillonite structures intercalated with Keggin cations and gibbsite-like polymers is in the character of the interlayer porosity. In Keggin cations, the height of pores is approximated by the height of the Keggin cations. Alternatively, in the most stable structure with gibbsite-like polymers, the height of pores is almost given by the height of Al-polymer rings, as shown in Figure 5.

ACKNOWLEDGMENTS

The authors are grateful to F. Leusen from Molecular Simulations for useful discussions. Support from the Grant Agency of the Czech Republic (grant no. 205/94/0468) and the Grant Agency of the Charles University, Prague (grant GAUK-33), is also acknowledged.

REFERENCES

Čapková P, Driessen RAJ, Numan M, Schenk H, Weiss Z, Klika Z. 1998. Molecular simulations of the montmorillonite intercalated with aluminum complex cations. Part I. Intercalation with $Al_{13}^{(7-x)+}$. Clays Clay Miner 46:232–239.

Driessen RAJ, Loopstra BO, de Bruijn DP, Kuipers HPCE, Schenk H. 1988. Program PLUVA. J Computer-Aided Molecular Design 2:225–240.

Dubbin WE, Goh TB, Oscarson DW, Hawthorne FC. 1994. Properties of hydroxy-Al and -Cr interlayers in montmorillonites. Clays Clay Miner 42:331–336.

Figueras F, Klapyta Z, Massiani P, Mountassir Z, Tichit D, Fajula F. 1990. Use of competitive ion exchange for intercalation of montmorillonite with hydroxy-aluminum species. Clays Clay Miner 38:257–264.

Hsu PH. 1988. Mechanism of gibbsite crystallization from partially neutralized aluminum chloride solutions. Clays Clay Miner 36:25–30.

Hsu PH. 1992. Reaction of OH-Al polymers with smectites and vermiculites. Clays Clay Miner 40:300–305.

Méring J, Oberlin A. 1967. Electron-optical study of smectites. Clay Clay Miner 27:3–18.

Plee D, Gatineau L, Fripiat JJ. 1987. Pillaring processes of smectites with and without tetrahedral substitution. Clays Clay Miner 35:81–88.

Saalfeld H, Wedde M. 1974. Refinement of the crystal structure of gibbsite $Al(OH)_3$. Zeitschrift fur Kristallografie 139: 129–135.

Schoonheydt RA, Leeman H. 1992. Pillaring of saponite in concentrated medium. Clay Miner 27:249–252.

Schoonheydt RA, Van den Eynde J, Tubbax H, Leeman H, Stuyckens M, Lenotte I, Stone WEE. 1993. The Al pillaring of clays. Part I. Pillaring with dilute and concentrated Al solutions. Clays Clay Miner 41:598–607.

Schoonheydt RA, Leeman H, Scorpion A, Lenotte I, Grobet P. 1994. The Al pillaring of clays. Part II. Pillaring with $[Al_{13}O_4(OH)_{24}(H_2O)_{12}]^{7+}$. Clays Clay Miner 42:518–525.

Tsipursky SI, Drits VA. 1984. The distribution of octahedral cations in 2:1 layers of dioctahedral smectites studied by oblique-texture electron diffraction. Clay Miner 19:177–193.

(Received 29 May 1996; accepted 9 August 1997; Ms. 2778, Part II)

https://doi.org/10.1346/CCMN.1998.0460303 Published online by Cambridge University Press